On the Role of Fresnel Factors in Sum-Frequency Generation Spectroscopy of Metal–Water and Metal-Oxide–Water Interfaces

Ellen H. G. Backus,*[,†,‡] Nuria Garcia-Araez,[†] Mischa Bonn,[†,‡] and Huib J. Bakker[†]

[†]FOM Institute AMOLF, Science Park 104, 1098 XG Amsterdam, The Netherlands

[‡]Max Planck Institute for Polymer Research, Ackermannweg 10, 55128 Mainz, Germany

ABSTRACT: We performed sum-frequency generation (SFG) spectroscopic measurements on water in contact with supported thin metal and metal-oxide films. We employed an internal reflection configuration and varied the angles of incidence of the visible and infrared beams and measured the SFG signals using different polarization combinations. While SFG is a surface-specific vibrational spectroscopy, the shape of the SFG spectra can be fully accounted for by the bulk response of the materials through the frequency-dependent enhancement of the local incident infrared fields at the interface, i.e., Fresnel effects. We find that the dispersion of the refractive index of the bulk water phase leads to a strong enhancement of the electric field at the interface at specific infrared frequencies. These local, frequency-dependent fields act on the frequency-independent, nonresonant SFG response of the electrons at the surfaces of the metal or metal-oxide films. As a result, the measured SFG spectra closely follow this infrared frequency dependence. Hence, we conclude that the nonresonant SFG signal from the electrons in the metal or metal-oxide film strongly dominates over the resonant SFG signal of the interfacial water vibrations. This work demonstrates the importance of Fresnel factors in SFG spectroscopy of metal(-oxide)–liquid interfaces and shows that the spectral dependence and magnitude of the Fresnel factors can be calculated, making corrections to the data in principle possible. Finally, this work provides practical recommendations for the selection of suitable experimental conditions for future SFG studies on metal(-oxide)–liquid interfaces aimed at elucidating interfacial water structures at these interfaces.

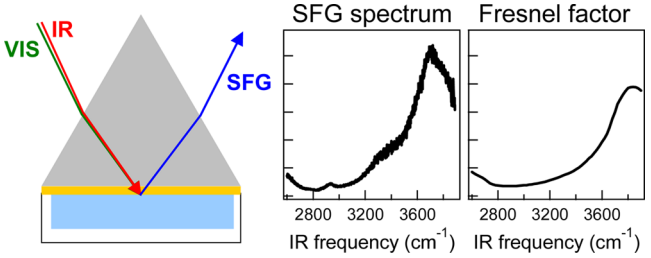

INTRODUCTION

The interaction of water with metal or metal-oxide surfaces plays a central role in many disciplines such as catalysis, electrochemistry, and biochemistry. Unfortunately, little is known about the properties of surface water on metals and metal-oxides, because in most techniques the signal of surface water is overwhelmed by the response of bulk water. Sum-frequency generation (SFG) provides high surface specificity and is thus an ideal technique to study the interface of water with a metal or metal-oxide. SFG is a second-order nonlinear optical process in which two light beams at frequencies ω_1 and ω_2 generate light at their sum frequency ($\omega_3 = \omega_1 + \omega_2$). The process of SFG is highly surface-specific, as the SFG process is forbidden in centrosymmetric media (within the electric dipole approximation). Hence, for centrosymmetric media like liquid water, SFG possesses monolayer interfacial specificity.

Typically, surface SFG experiments employ a pulsed visible laser beam of fixed wavelength and a pulsed tunable infrared laser beam. The sum-frequency signal is enhanced when the infrared frequency matches a vibrational resonance of some interfacial species. Thus, by recording the SFG signal as a function of the infrared frequency, one can obtain an SFG spectrum which contains unique information on the vibrational response of the surface molecules. Surface or interfacial SFG has been widely employed in surface science studies.[1−17]

In spite of the inherent power of surface SFG, the interpretation of surface SFG spectra is unfortunately often not straightforward. One complication is that the measured SFG signal not only consists of the signal originating from the interfacial vibrational resonances but also contains a nonresonant contribution. This nonresonant contribution originates from the nonlinear susceptibility associated with nonresonant but potentially strong electronic transitions. The resonant and the nonresonant sources of SFG radiation interfere. As a result, depending on the relative strengths of the two contributions, a variety of different SFG band-shapes may appear, such as monopolar, bipolar, or inverted bands.[18−20]

Another complication is that the SFG signal depends on the magnitude of the local electric fields of the three interacting optical beams at the interface. The local electric field strengths depend not only on the intensity of the incident beams but also on the bulk, linear refractive indices of the different layers of the sample, in a manner described by the Fresnel factors. These effects are particularly relevant for the infrared beam, as one or both of the bulk phases bordering the interface may display strong dispersion in the infrared frequency region. As such, it

has been shown that the correct interpretation of SFG spectra requires the evaluation of Fresnel factors.[21−30] In the present work, we show that this is especially true for SFG measurements performed on thin metal and metal-oxide films in contact with a bulk liquid, because of the strong nonresonant second-order nonlinear response of the metal(-oxide).

We present a detailed analysis of the SFG spectra of thin films of gold, titanium (Ti), and indium tin oxide (ITO) in contact with water. We performed measurements and calculations under different polarization combinations for the infrared, visible, and sum-frequency light and at different angles of incidence of the visible and infrared beams. It is shown that the Fresnel factors exhibit a marked frequency-dependence due to the frequency-dependence of the refractive index of bulk water in the infrared region. We find that the Fresnel effects give rise to a strong spectral structuring of the SFG signal that can easily be confused for the presence of particular interfacial vibrational resonances. Moreover, we show that due to the Fresnel factors the SFG signal at a certain polarization combination can be amplified by several orders of magnitude in comparison to the SFG signal obtained at other polarization combinations, especially for water−metal interfaces.

THEORY

The basic theory of SFG has been described elsewhere.[29,31] Briefly, the SFG intensity, I_{SFG}, is proportional to the intensities of the incident visible and infrared beams, I_{VIS} and I_{IR}, and to the square of the second-order nonlinear susceptibilities, $\chi^{(2)}_{ijk}(\omega_{SFG} = \omega_{VIS} + \omega_{IR})$, of the interface

$$I_{SFG}(\omega_{SFG}) \propto \left|\sum_{i,j,k} L_{ii}(\omega_{SFG})\chi^{(2)}_{ijk}(\omega_{SFG} = \omega_{VIS} + \omega_{IR})L_{jj}(\omega_{VIS})L_{kk}(\omega_{IR})\right|^2 \sec^2\theta_{SFG} I_{VIS} I_{IR} \quad (1)$$

where i, j, k (= x, y, or z) are the coordinates of the reference frame defined in Figure 1; L_{ii}, L_{jj}, and L_{kk} are the Fresnel

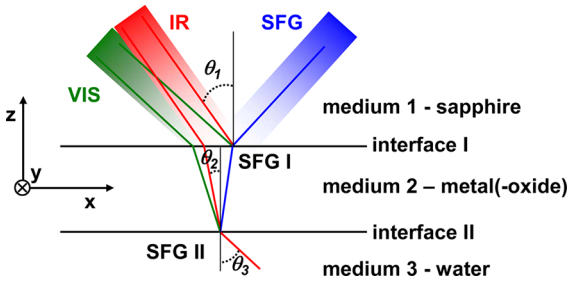

Figure 1. Sketch of SFG from a model sapphire−metal(-oxide)−water layer. For simplicity, multiple reflections of the beams are not shown.

coefficients or local field factors, which define the magnitude of the electric fields at the interface (in relation to the magnitude of the electric fields of the incident beams); and θ_{SFG} is the reflected angle of the SFG beam (with respect to the surface normal) in medium 1. Equation 1 illustrates the essence of the challenge addressed in this manuscript: the quantity $\chi^{(2)}_{ijk}(\omega_{SFG} = \omega_{VIS} + \omega_{IR})$ possesses resonant character due to the vibrational response of the interface, but its frequency dependence can easily be concealed by the frequency dependence of the Fresnel coefficients $L(\omega)$. For readability we omit in the remainder of this manuscript the explicit frequency dependence of $\chi^{(2)}_{ijk}$.

For a thin film in between two media, e.g., sapphire and water (Figure 1), the SFG signal will be generated at both the sapphire-film and the film-water interfaces. Consequently, the total SFG intensity is given by the sum of two contributions

$$I_{SFG}(\omega_{SFG}) \propto \left|\sum_{i,j,k} L^{I}_{ii}(\omega_{SFG})\chi^{(2),I}_{ijk}L^{I}_{jj}(\omega_{VIS})L^{I}_{kk}(\omega_{IR}) + \sum_{i,j,k} L^{II}_{ii}(\omega_{SFG})\chi^{(2),II}_{ijk}L^{II}_{jj}(\omega_{VIS})L^{II}_{kk}(\omega_{IR})\right|^2 \sec^2\theta_{SFG} I_{VIS} I_{IR} \quad (2)$$

where the superscripts I and II refer to the interface between media 1 and 2 and between media 2 and 3, respectively (Figure 1). For each interface, 7 of the 27 elements of the third-rank tensor $\chi^{(2)}_{ijk}$ are nonzero, of which 4 can have a different value.[29,31] In this work we perform SFG measurements under four different polarization combinations of the SFG, visible (VIS), and infrared (IR) beams: SSP (referring to S-polarized SFG, S-polarized VIS, and P-polarized IR), SPS, PSS, and PPP. The corresponding SFG intensities can be expressed as[29,31]

$$I_{SFG,SSP}(\omega_{SFG}) \propto \left|\sum_n L^n_{yy}(\omega_{SFG})L^n_{yy}(\omega_{VIS})L^n_{zz}(\omega_{IR})\sin\theta_{IR}\chi^{(2),n}_{yyz}\right|^2 \sec^2\theta_{SFG} I_{VIS} I_{IR} \quad (3a)$$

$$I_{SFG,SPS}(\omega_{SFG}) \propto \left|\sum_n L^n_{yy}(\omega_{SFG})L^n_{zz}(\omega_{VIS})L^n_{yy}(\omega_{IR})\sin\theta_{VIS}\chi^{(2),n}_{yzy}\right|^2 \sec^2\theta_{SFG} I_{VIS} I_{IR} \quad (3b)$$

$$I_{SFG,PSS}(\omega_{SFG}) \propto \left|\sum_n L^n_{zz}(\omega_{SFG})L^n_{yy}(\omega_{VIS})L^n_{yy}(\omega_{IR})\sin\theta_{SFG}\chi^{(2),n}_{zyy}\right|^2 \sec^2\theta_{SFG} I_{VIS} I_{IR} \quad (3c)$$

$$I_{SFG,PPP}(\omega_{SFG}) \propto \left|\sum_n \left(- L^n_{xx}(\omega_{SFG})L^n_{xx}(\omega_{VIS})L^n_{zz}(\omega_{IR}) \cos\theta_{SFG}\cos\theta_{VIS}\sin\theta_{IR}\chi^{(2),n}_{xxz} - L^n_{xx}(\omega_{SFG}) L^n_{zz}(\omega_{VIS})L^n_{xx}(\omega_{IR})\cos\theta_{SFG}\sin\theta_{VIS}\cos\theta_{IR}\chi^{(2),n}_{xzx} + L^n_{zz}(\omega_{SFG})L^n_{xx}(\omega_{VIS})L^n_{xx}(\omega_{IR})\sin\theta_{SFG}\cos\theta_{VIS} \cos\theta_{IR}\chi^{(2),n}_{zxx} + L^n_{zz}(\omega_{SFG})L^n_{zz}(\omega_{VIS})L^n_{zz}(\omega_{IR}) \sin\theta_{SFG}\sin\theta_{VIS}\sin\theta_{IR}\chi^{(2),n}_{zzz}\right)\right|^2 \sec^2\theta_{SFG} I_{VIS} I_{IR} \quad (3d)$$

where n denotes either one of the two interfaces (I and II) and θ_{IR} and θ_{VIS} are the incident angles of the infrared and visible beams in medium 1 (with respect to the surface normal; see Figures 1 and 2).

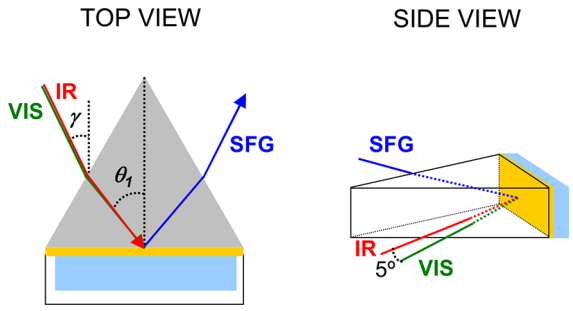

Figure 2. Top (left) and side (right) view of the experimental setup. Orange and blue represent the metal(-oxide) and water layer, respectively.

The Fresnel coefficients of a model three-layer system, with and without multiple reflections in the second layer, have been reported previously in literature.[21,23−26,30,32] The expressions for the Fresnel coefficients involve the complex refractive indexes of the different components of the system.[28,33] We follow the notation of ref 30, as we have the same system: practically copropagating incoming beams, SFG detected in reflection, and multiple reflections in the thin metal(-oxide) film.[34] The precise form of the Fresnel factor depends on the definition of $\chi^{(2)}_{ijk}$. We choose to follow the general convention[32,35] where the polarization sheet and thus the generated sum-frequency field is placed outside the nonlinear medium, and the incoming electric fields are defined just inside the nonlinear medium. Following ref 30 and this definition, we get the following Fresnel factors. The equations are derived by considering that the boundaries separating the layers are plane and parallel.

The Fresnel factors of interface I (i.e., the sapphire−metal(-oxide) interface) are given by

$$L^{\mathrm{I}}_{xx}(\omega) = \frac{t^{\mathrm{p}}_{12}}{1 + r^{\mathrm{p}}_{12} r^{\mathrm{p}}_{23} \mathrm{e}^{2i\beta}}(1 - r^{\mathrm{p}}_{23}\mathrm{e}^{2i\beta})\frac{\cos\theta_2}{\cos\theta_1} \tag{4a}$$

$$L^{\mathrm{I}}_{yy}(\omega) = \frac{t^{\mathrm{s}}_{12}}{1 + r^{\mathrm{s}}_{12} r^{\mathrm{s}}_{23} \mathrm{e}^{2i\beta}}(1 + r^{\mathrm{s}}_{23}\mathrm{e}^{2i\beta}) \tag{4b}$$

$$L^{\mathrm{I}}_{zz}(\omega) = \frac{t^{\mathrm{p}}_{12}}{1 + r^{\mathrm{p}}_{12} r^{\mathrm{p}}_{23} \mathrm{e}^{2i\beta}}(1 + r^{\mathrm{p}}_{23}\mathrm{e}^{2i\beta})\frac{n_1 n_2}{n_{\mathrm{interfaceI}}{}^2} \tag{4c}$$

where ω is the beam frequency and $n_{\mathrm{interfaceI}}$ is equal to n_1 or n_2 (as will be explained below); n_1 and n_2 are the complex refractive indices of medium 1 (sapphire) and medium 2 (metal(-oxide)). r^{p}_{ij}, r^{s}_{ij}, t^{p}_{ij}, and t^{s}_{ij} are the linear transmission and reflection coefficients at the boundary between media i and j, for p- or s-polarized light

$$r^{\mathrm{p}}_{ij} = \frac{n_j \cos\theta_i - n_i \cos\theta_j}{n_j \cos\theta_i + n_i \cos\theta_j} \tag{5a}$$

$$r^{\mathrm{s}}_{ij} = \frac{n_i \cos\theta_i - n_j \cos\theta_j}{n_i \cos\theta_i + n_j \cos\theta_j} \tag{5b}$$

$$t^{\mathrm{p}}_{ij} = \frac{2n_i \cos\theta_i}{n_j \cos\theta_i + n_i \cos\theta_j} \tag{5c}$$

$$t^{\mathrm{s}}_{ij} = \frac{2n_i \cos\theta_i}{n_i \cos\theta_i + n_j \cos\theta_j} \tag{5d}$$

θ_1 and θ_2 (see Figure 1) are the beam incident angles in medium 1 (sapphire) and medium 2 (metal(-oxide)), measured with respect to the surface normal. β, in eq 4 is a phase difference factor, given by

$$\beta = \frac{2\pi}{\lambda} n_2 d \cos\theta_2 \tag{6}$$

where λ is the beam wavelength and d is the thickness of medium 2 (thin metal(-oxide) film). As n_2 is complex, β will be complex as well.

The Fresnel eqs 4a−4c are valid both for the incoming IR/VIS field and for the reflected SFG beam.[21] However, the L_{zz} component will be different for an incoming or outgoing beam, because $\chi^{(2)}_{ijk}$ assumes the incoming fields to be placed in the nonlinear medium, and the polarization sheet and thus the generated sum-frequency field to be placed just outside the medium. This difference is expressed in the value taken for $n_{\mathrm{interfaceI}}$. In general the $\chi^{(2)}_{ijk}$ for sapphire (medium 1) is much smaller than that of the metal(-oxide) (medium 2), so that the nonlinear medium (i.e., the medium with the largest nonlinear optical response) will be medium 2. Hence in L^{I}_{zz}, for the incoming IR and VIS beams $n_{\mathrm{interfaceI}} = n_2$. In our definition, in which the nonlinear polarization source is placed outside the nonlinear medium, the nonlinear source is thus placed in medium 1, resulting in $n_{\mathrm{interfaceI}} = n_1$ for the outgoing SFG field. The difference between $L^{\mathrm{I}}_{zz,\mathrm{SFG}}$ and $L^{\mathrm{I}}_{zz,\mathrm{VIS/IR}}$ is just a factor $(n_1/n_2)^2$ originating from the displacement rather than the field being continuous in the z direction, which follows from the Maxwell equations.[36] If $\chi^{(2)}_{ijk}$ for medium 1 would be larger than for medium 2, then for the incoming fields $n_{\mathrm{interfaceI}} = n_1$ and for the resulting SFG $n_{\mathrm{interfaceI}} = n_2$.

For interface II (metal(-oxide)−water) the Fresnel factors read[37]

$$L^{\mathrm{II}}_{xx}(\omega) = \mathrm{e}^{i\Delta}\frac{t^{\mathrm{p}}_{12}}{1 + r^{\mathrm{p}}_{12} r^{\mathrm{p}}_{23} \mathrm{e}^{2i\beta}}(1 - r^{\mathrm{p}}_{23})\frac{\cos\theta_2}{\cos\theta_1} \tag{7a}$$

$$L^{\mathrm{II}}_{yy}(\omega) = \mathrm{e}^{i\Delta}\frac{t^{\mathrm{s}}_{12}}{1 + r^{\mathrm{s}}_{12} r^{\mathrm{s}}_{23} \mathrm{e}^{2i\beta}}(1 + r^{\mathrm{s}}_{23}) \tag{7b}$$

$$L^{\mathrm{II}}_{zz}(\omega) = \mathrm{e}^{i\Delta}\frac{t^{\mathrm{p}}_{12}}{1 + r^{\mathrm{p}}_{12} r^{\mathrm{p}}_{23} \mathrm{e}^{2i\beta}}(1 + r^{\mathrm{p}}_{23})\frac{n_1 n_2}{n_{\mathrm{interfaceII}}{}^2} \tag{7c}$$

where $n_{\mathrm{interfaceII}}$ is equal to n_2 or n_3. The factor $\mathrm{e}^{i\Delta}$ takes into account the phase difference between SFG generated at interface I and II (and thus the absorption in medium 2) and is present for both the incoming IR/VIS and outgoing SFG field, but with a different Δ. The definitions for Δ read[23,26,30]

$$\Delta_{\mathrm{SFG}} = \frac{2\pi n_{2,\mathrm{SFG}} d}{\lambda_{\mathrm{SFG}} \cos\theta_{2,\mathrm{SFG}}} \tag{8a}$$

$$\Delta_{\mathrm{VIS}} = \frac{2\pi n_{2,\mathrm{VIS}} d}{\lambda_{\mathrm{VIS}} \cos\theta_{2,\mathrm{VIS}}} - \frac{2\pi n_{1,\mathrm{VIS}} d}{\lambda_{\mathrm{VIS}}}(\tan\theta_{2,\mathrm{VIS}} + \tan\theta_{2,\mathrm{SFG}})\sin\theta_{1,\mathrm{VIS}} \tag{8b}$$

$$\Delta_{\mathrm{IR}} = \frac{2\pi n_{2,\mathrm{IR}} d}{\lambda_{\mathrm{IR}} \cos\theta_{2,\mathrm{IR}}} - \frac{2\pi n_{1,\mathrm{IR}} d}{\lambda_{\mathrm{VIS}}}(\tan\theta_{2,\mathrm{IR}} + \tan\theta_{2,\mathrm{SFG}})\sin\theta_{1,\mathrm{IR}} \tag{8c}$$

As for the first interface (sapphire−metal(-oxide)), the Fresnel factors for the second interface (metal(-oxide)−water) in eq 7 are valid both for the incoming IR/VIS fields and the outgoing SFG beam, the difference being contained in the definition for $n_{\text{interfaceII}}$. In case the $\chi^{(2)}_{ijk}$ of medium 2 is much larger than that of medium 3, then for the incoming IR/VIS field $n_{\text{interfaceII}} = n_2$ and for the resulting SFG $n_{\text{interfaceII}} = n_3$. The opposite definition is valid in case $\chi^{(2)}_{ijk}$ of medium 3 is much larger than that of medium 2: for the IR/VIS field $n_{\text{interfaceII}} = n_3$ and for the resulting SFG $n_{\text{interfaceII}} = n_2$. Also here, the difference between the Fresnel factor for the incoming and outgoing beam is a factor $(n_2/n_3)^2$ owing to the displacement being continuous.

In the above given Fresnel factors the transmission from air into the sapphire prism for the incoming beams and the transmission from sapphire to air for the SFG is not taken into account, as this factor is not frequency dependent in the IR region. Of course, the refraction at the air-prism interface is taken into account (see the Experimental Section). Moreover, to avoid calculating with complex angles (θ_1 is real as the refractive index of our medium 1 (sapphire) is real in the frequency range used in this paper), we make the following substitution in eqs 4a, 5, 6, 7a and 8[38]

$$\cos\theta_j = \frac{\sqrt{n_j^2 - n_1^2 \sin^2\theta_1}}{n_j} \tag{9}$$

Equation 9 and Snell's law are used to convert the tan θ_2 terms of eq 8 into terms containing only sin θ_1.

EXPERIMENTAL SECTION

Figure 2 shows a schematic outline of the experimental setup. The sample is a thin metal or metal-oxide layer deposited on a sapphire equilateral prism (face dimension: 10 by 14 mm), put in contact with pure water H_2O (Millipore, 18.2 MΩ cm) or D_2O (Merck, 99.9%). The sample cell is made of Teflon and allows the exchange of the solution without affecting the optical alignment. The deposits of gold and titanium were made by electron beam evaporation at a base pressure $<2 \times 10^{-6}$ mbar. The final thickness of the layer was monitored with a quartz microbalance. The ITO layer (In_2O_3/SnO_2, 90/10 wt %) was prepared by magnetron sputtering.[39]

The SFG experiments were carried out in a copropagating internal reflection geometry, because the strong vibrational absorption of the liquid would complicate the performance of SFG spectroscopy from the liquid side (external-reflection geometry). The SFG light is detected in reflection. To perform experiments in an internal reflection configuration, it is necessary to prepare very thin metal films as most metals are very strong absorbers of visible and infrared light. Indeed, previous SFG measurements in the internal reflection configuration could not detect the presence of adsorbates on gold thin films of thickness larger than 5−10 nm.[40] On the other hand, very thin metal films are known to contain a lot of pores, meaning that the sapphire-water interface will also contribute to the signal. We used a minimal layer thickness of 5 nm. Although there might still be pores present they will not contribute significantly to the signal: the SFG signal from a bare prism is at least 2 orders of magnitude lower than the signal from a prism with a metal(-oxide) layer. As ITO is not as strongly absorbing as the metals, we could use a thicker layer of this material. We performed experiments for gold, titanium, and ITO layers with thicknesses of 5, 5, and 100 nm, respectively.

The incident angles of the visible and infrared beams, γ_{VIS} and γ_{IR}, were varied by rotating the prism around its primary axis. The values of γ_{VIS} and γ_{IR} were measured from the directions of the beams outside the prism (with respect to the central plane of symmetry of the prism). The internal incident angles at the sapphire-metal interface, $\theta_{1,\text{VIS}}$ and $\theta_{1,\text{IR}}$, were calculated from the refraction at the air-sapphire interface (see Figure 2). In our experiments, the incident angles of the visible and infrared beams were equal, and the azimuthal angles differed by about 5° (see Figure 2). The narrow-band visible beam was obtained by passing part of the output of a ∼100 fs amplified Ti:sapphire laser system (Legend, Coherent, Inc.) through an etalon. This beam had a central wavelength of ∼800 nm, an energy of ∼20 μJ/pulse, and a bandwidth of 17 cm^{-1}. The infrared pulses were generated by an OPG/OPA (TOPAS, Light Conversion) system pumped by another part of the output of the laser system. The infrared pulses had an energy of ∼5 μJ/pulse and a bandwidth of 150 cm^{-1}. In order to study a broad infrared frequency window, the measurements were performed by sweeping the infrared frequency using the automated control of the TOPAS motors of the grating, delay lines and the crystal rotator. In order to minimize the absorption of the infrared pulses by water vapor, the chamber covering the infrared beam was continuously purged with N_2. The infrared and visible beams were focused loosely at the sample down to a beam waist diameter of ∼5 mm, to avoid damaging of the thin metal(-oxide) films. The reflected SFG light was spectrally dispersed by a monochromator and detected by an electron-multiplied charge coupled device (EMCCD, Andor Technologies). The acquisition time was varied between 60 and 300 s per spectrum, depending on the signal size. Prior to the experiments, the thin film deposits were cleaned with acetone and isopropanol and by thorough rinsing with ultrapure water. The Teflon cell and all the glassware were immersed overnight in a concentrated solution of slightly acidic $KMnO_4$. The residual $KMnO_4$ was removed with a diluted solution of H_2O_2 and sulfuric acid (3:1). Finally the cell was thoroughly washed with ultrapure water.

To obtain SFG spectra, the measured SFG intensity has to be corrected for the frequency-dependent IR intensity. In previous work, this normalization is done by measuring the SFG spectrum from a nonresonant reference sample (such as z-cut quartz). However, the experiments described here involve thin metal films supported on a sapphire prism, and as a result, the temporal and spatial overlap of the visible and infrared beams for SFG generation are not the same as in the case of the air−quartz interface. Consequently, in order to perform an accurate normalization of the SFG intensities, we performed successive SFG measurements with H_2O or D_2O as the water layer. The SFG signal obtained with D_2O constitutes the nonresonant reference measurement that is used to normalize the SFG signals obtained with H_2O. This approach is accurate, because all the experimental conditions (thin film, optical alignment, etc) are identical in the measurements with H_2O and D_2O. We checked that the spectra measured in H_2O and in D_2O are highly reproducible, even after several exchanges.

RESULTS AND DISCUSSION

Experimental SFG Spectra. Figure 3a shows the ratios of the SFG intensities measured for a 5 nm gold film in contact with H_2O and D_2O at different incident angles of the visible and infrared beams (γ = 22°, 43°, 60°, and 75°), using PPP polarization. Measurements performed with the bare sapphire

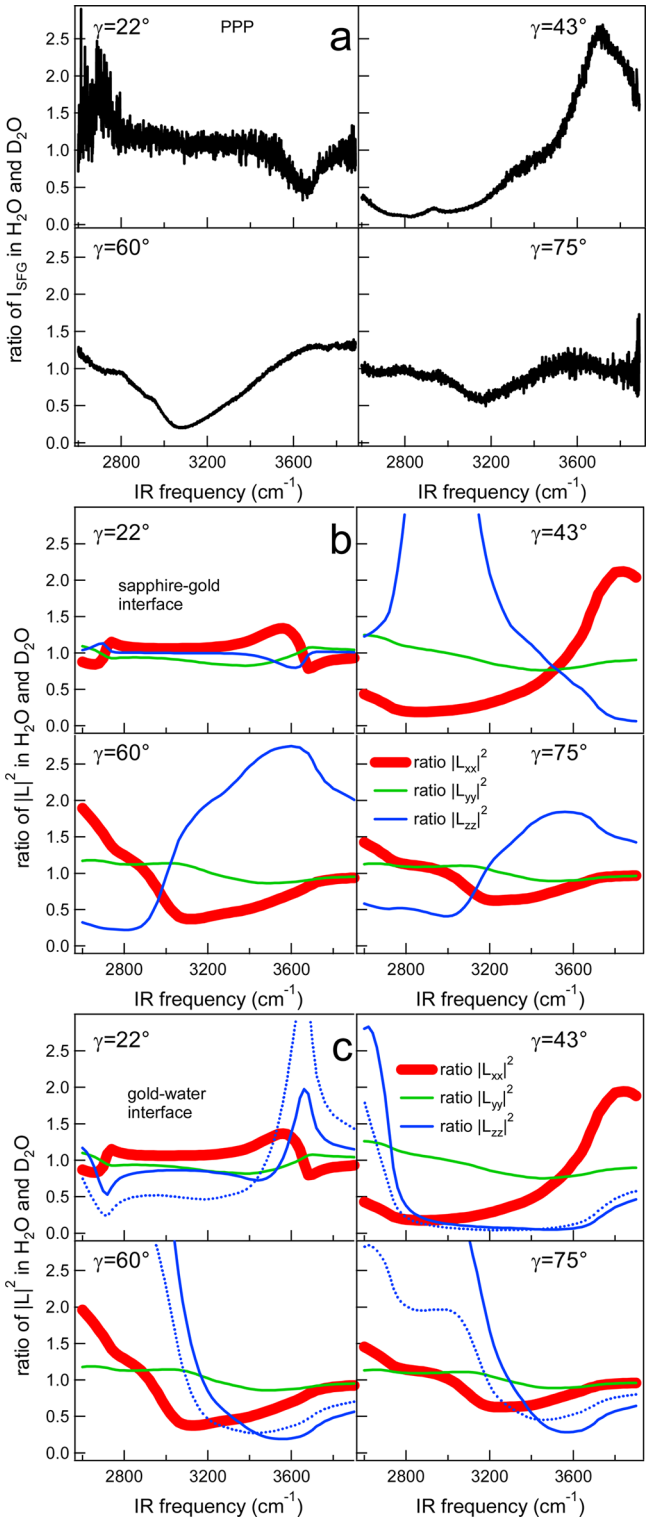

Figure 3. (a) Ratio of the SFG intensity measured in H_2O and in D_2O with gold as medium 2, for γ = 22, 43, 60, and 75° under PPP polarization. (b) Ratio of the square of the calculated IR Fresnel factors for H_2O and for D_2O $|L_{xx,H_2O}(\omega_{IR})|^2/|L_{xx,D_2O}(\omega_{IR})|^2$ (red), $|L_{yy,H_2O}(\omega_{IR})|^2/|L_{yy,D_2O}(\omega_{IR})|^2$ (green), and $|L_{zz,H_2O}(\omega_{IR})|^2/|L_{zz,D_2O}(\omega_{IR})|^2$ (blue) for the sapphire-gold interface. (c) Like b but for the gold-water interface. The blue solid and dotted line represent the case for $\chi^{(2)}_{gold} > \chi^{(2)}_{water}$ and $\chi^{(2)}_{water} > \chi^{(2)}_{gold}$, respectively. The thick lines in panel b and c represent the strongest calculated Fresnel factor for the chosen polarization combination in the experiment.

prism (i.e., without gold layer) showed that the SFG intensity was roughly 150 times smaller, demonstrating that the results in Figure 3a do not contain significant contributions from exposed sapphire resulting from holes in the gold layer. The signal size is strongly dependent on the incident angles, being large for 43 and 60°, and much smaller for 22° and 75°. We found no signal for SSP polarization. The signals measured for H_2O and D_2O are clearly different, resulting in a ratio different from 1. Previously, the differences in SFG response measured for H_2O and D_2O were ascribed to the vibrational resonances of interfacial H_2O molecules.[41,42] However, one would expect the resonant SFG signal for an H_2O interface to appear at frequencies near 3300 cm^{-1}. Figure 3a shows that the main differences in SFG intensity between H_2O and D_2O are found at significantly lower and higher frequencies than the expected 3300 cm^{-1} of the maximum of the absorption of the O−H stretch vibrations.

In Figure 4a the ratio of SFG signals obtained from a system with 5 nm titanium in contact with H_2O and D_2O is depicted for SSP and PSS polarization at 45°; the PSS signal is roughly 60 times larger than the SSP signal. Spectral modulations are observed at very low and very high frequencies (2700 and 3800 cm^{-1}), which do not correspond with the vibrational resonances of H_2O or D_2O. The signals for PPP and SPS (data not shown) are of similar strength as SSP, and the ratios look similar to SSP and PSS, respectively.

For a 100 nm ITO layer in contact with H_2O/D_2O, see Figure 5a, we again observe spectral features at frequencies that do not correspond to the vibrational resonances of H_2O and D_2O. The ITO film shows a roughly 6 times larger signal for SSP than for PPP.

Table 1 summarizes the signal sizes for the different systems measured. Due to the difficulties in the normalization described in the experimental part, only the relative signal sizes between the different polarization combinations for each system (i.e., SSP vs PPP for ITO or the different signals of titanium) are presented. For the different systems the polarization combination that gives the largest signal differs: for ITO the signal is extremely large for the SSP polarization configuration, while for gold the signal obtained with SSP is very small (below the detection limit).

Clearly, the three systems show very different SFG responses, but have in common that the spectra do not contain clear features that can be assigned to the OH stretch vibrations of interfacial H_2O. Apparently we do not measure the resonant signal from interfacial water but rather a nonresonant (NR) signal most likely originating from the metal(-oxide) layer. Surprisingly, the metal and metal-oxide interfaces do not induce a structuring of the water that would lead to a significant SFG signal. The resonant SFG signal seems to be orders of magnitude smaller than the NR signal from the metal(-oxide). Unfortunately, it is not possible to suppress this NR signal with respect to the resonant signal by introducing a time-delay between the visible and infrared pulse,[43] because the water molecules at the interface show a very short dephasing time. The NR signal has a strong frequency dependence, which originates from the Fresnel factors, as shown in the following.

Calculation Results. We calculate the Fresnel factors of the studied systems using the equations given in the Theory section. To allow a direct comparison with the experiments, we calculate the ratio of the Fresnel factors for the systems with H_2O and D_2O. We assume the layers to be perfectly flat; we do not take account for the corrugated structure of the metal films.

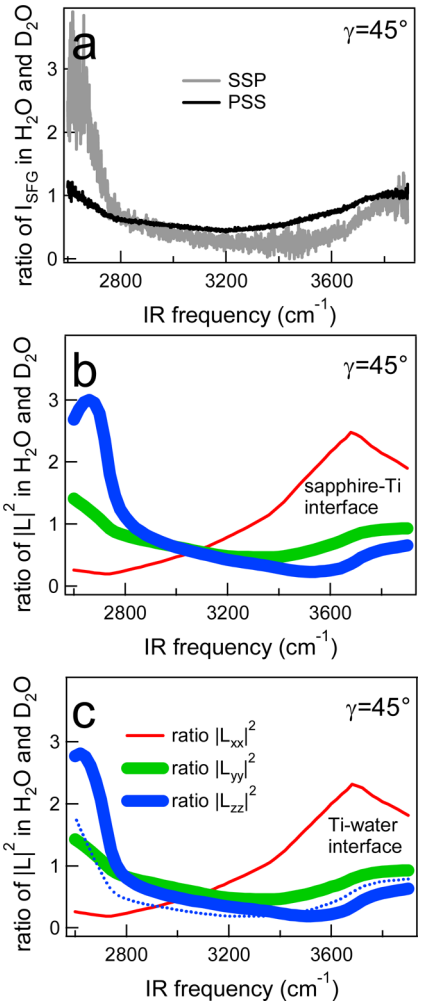

Figure 4. (a) Ratio of the SFG intensity measured in H_2O and in D_2O with titanium (Ti) as medium 2 under SSP and PSS polarization for γ = 45°. (b) Ratio of the square of the calculated IR Fresnel factors for H_2O and for D_2O $|L_{xx,H_2O}(\omega_{IR})|^2/|L_{xx,D_2O}(\omega_{IR})|^2$ (red), $|L_{yy,H_2O}(\omega_{IR})|^2/|L_{yy,D_2O}(\omega_{IR})|^2$ (green), and $|L_{zz,H_2O}(\omega_{IR})|^2/|L_{zz,D_2O}(\omega_{IR})|^2$ (blue) for the sapphire-Ti interface. (c) Like b but for the Ti-water interface. The blue solid and dotted line represent the case for $\chi^{(2)}_{Ti} > \chi^{(2)}_{water}$ and $\chi^{(2)}_{water} > \chi^{(2)}_{Ti}$, respectively. The thick lines in panel b and c represent the strongest calculated Fresnel factor for the chosen polarization combination in the experiment.

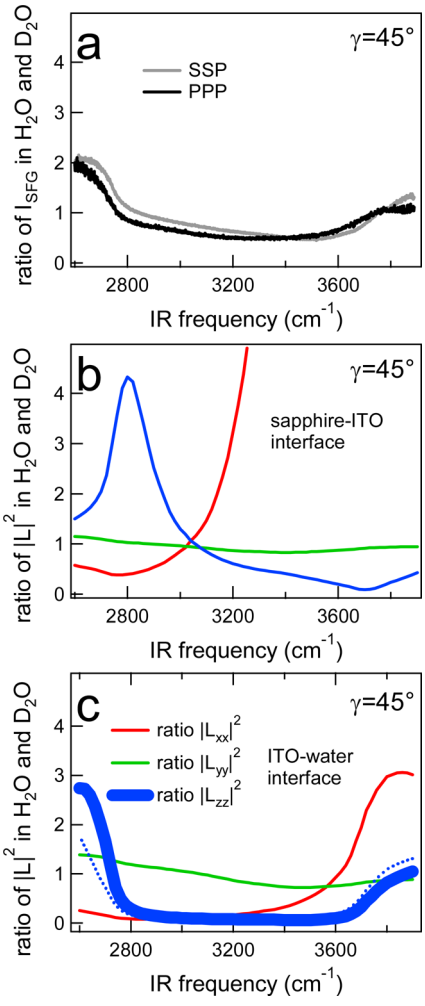

Figure 5. (a) Ratio of the SFG intensity measured in H_2O and in D_2O with ITO as medium 2 under SSP and PPP polarization for γ = 45°. (b) Ratio of the square of the calculated IR Fresnel factors for H_2O and for D_2O $|L_{xx,H_2O}(\omega_{IR})|^2/|L_{xx,D_2O}(\omega_{IR})|^2$ (red), $|L_{yy,H_2O}(\omega_{IR})|^2/|L_{yy,D_2O}(\omega_{IR})|^2$ (green), and $|L_{zz,H_2O}(\omega_{IR})|^2/|L_{zz,D_2O}(\omega_{IR})|^2$ (blue) for the sapphire-ITO interface. (c) Like b but for the ITO-water interface. The blue solid and dotted line represent the case for $\chi^{(2)}_{ITO} > \chi^{(2)}_{water}$ and $\chi^{(2)}_{water} > \chi^{(2)}_{ITO}$, respectively. The thick line in panel c represents the strongest calculated Fresnel factor for the chosen polarization combination in the experiment.

When calculating the spectral shape we only consider the Fresnel factors for the infrared light and not for the SFG light, as there is very little dispersion at the SFG frequency. The visible light is narrow-band and can therefore not produce any frequency dependence. We use the optical constants of sapphire from ref 44 and for H_2O and D_2O from ref 45. The optical constants for water in the visible are taken from ref 46. The small birefringence (0.008) of sapphire is not taken into account as we found no experimental evidence that it plays a significant role: e.g. for the titanium-water interface the (forbidden) SSS polarization signal is roughly 20 times smaller than the PSS signal, indicating only very small amount of rotation of the polarizations. The refractive indices of gold and of titanium are taken from ref 44 and the refractive index of the metal-oxide ITO is obtained from ref 47. We calculate the ratio of the square of the Fresnel factors for the sapphire–metal(-oxide) and metal(-oxide)–water interface both for the case that the signal would originate from the metal(-oxide) layer, and for the case that the signal would originate from the sapphire and/or water layer, i.e., $\chi^{(2)}_{metal(-oxide)} > \chi^{(2)}_{water/sapphire}$ and $\chi^{(2)}_{water/sapphire} > \chi^{(2)}_{metal(-oxide)}$. The only difference between the two cases is the value for $n_{interface}$ which is only present in L^n_{zz}.

Table 1. Relative Signal Sizes for the Different Experimental Systems and Geometries

	gold 5 nm				Ti 5 nm	ITO 100 nm
	22°	43°	60°	75°	45°	45°
SSP	0	0	0	0	small 1*PPP	very large 6*PPP
SPS					small 2*PPP	
PSS					large 60*PPP	
PPP	small	large	large	small	small	large

Hence, L^n_{xx} and L^n_{yy} will be equal for the two cases and thus the ratios $L^n_{xx,H_2O}(\omega_{IR})/L^n_{xx,D_2O}(\omega_{IR})$ and $L^n_{yy,H_2O}(\omega_{IR})/L^n_{yy,D_2O}(\omega_{IR})$ remain the same. For L^I_{zz}, $n_{interface}$ is either $n_{metal(-oxide)}$ or $n_{sapphire}$. For the ratio $L^I_{zz,H_2O}(\omega_{IR})/L^I_{zz,D_2O}(\omega_{IR})$, the two cases are identical, as $n_{interfaceI}$ in eq 4c will cancel out in the ratio; both H_2O and D_2O have the same $n_{interfaceI}$. However, for interface II this is not the case. If the metal(-oxide) film is the predominant source of the nonresonant nonlinear response, $n_{interfaceII}$ will still cancel in the ratio as the metal(-oxide) is the nonlinear medium both for the system with H_2O and for the system with D_2O. However, if water is the (resonant or nonresonant) nonlinear medium $n_{interfaceII}$ will not cancel as $n_{interfaceII} = n_{H_2O}$ for the system with H_2O and $n_{interfaceII} = n_{D_2O}$ for the system with D_2O. Hence, the ratio $L^{II}_{zz,H_2O}(\omega_{IR})/L^{II}_{zz,D_2O}(\omega_{IR})$ is determined by the nature of the nonlinear medium. The value of $n_{interface}$ has a strong effect on the amplitude of the Fresnel factors, especially in the case of gold, i.e., a material with a very high refractive index. This effect is divided out when we consider the ratio of the Fresnel factors of the H_2O and D_2O systems. The Fresnel factors do not include any resonant contribution from the interfacial water. These resonant contributions are represented by the frequency dependence of the resonant part of $\chi^{(2)}_{ijk}$ and are not considered in the present calculations.

The calculated ratios of the squared Fresnel factors are plotted in Figure 3–5 for the gold, titanium and ITO system, respectively. Figure 6 shows the square of the Fresnel factor $|L_{xx}|^2$ for both H_2O and D_2O (and not the ratio) for the system with gold as medium 2. Figure 6 shows that for D_2O the Fresnel factor shows strong frequency dependence below 3000 cm^{-1}, while for H_2O the Fresnel factor depends on frequency above 3000 cm^{-1}. By comparing all calculated ratios of the squared Fresnel factors, we find that for all systems the ratios $|L^I_{yy,H_2O}(\omega_{IR})|^2/|L^I_{yy,D_2O}(\omega_{IR})|^2$ and $|L^{II}_{yy,H_2O}(\omega_{IR})|^2/|L^{II}_{yy,D_2O}(\omega_{IR})|^2$ have approximately the same shape and have a ratio around 1 at all frequencies. The ratios for the $L^n_{xx}(\omega_{IR})$ and $L^n_{zz}(\omega_{IR})$ depend more strongly on the frequency and on the particular system, because the linear transmission and reflection coefficients (eq 5) for p-polarized light, especially r^p_{23}, are more strongly frequency modulated compared to the transmission and reflection coefficients for s-polarized light which are present in the $L^n_{yy}(\omega_{IR})$ Fresnel factors. We notice that for the titanium film $|L^I_{nn,H_2O}(\omega_{IR})|^2/|L^I_{nn,D_2O}(\omega_{IR})|^2$ is equal to $|L^{II}_{nn,H_2O}(\omega_{IR})|^2/|L^{II}_{nn,D_2O}(\omega_{IR})|^2$ ($nn = xx, yy, zz$). This result has its origin in the almost zero value for β and Δ making the expression for $L^I_{nn}(\omega_{IR})$ and $L^{II}_{nn}(\omega_{IR})$ equal (see eqs 4 and 7). In contrast, for ITO β is large, mainly because of the 20 times thicker film, resulting in a large difference between the Fresnel factors of the first and the second interface. For all systems, the imaginary parts of β and Δ become large for very thick layers, due to absorption in the film. Hence, the terms $e^{2i\beta}$ and $e^{i\Delta}$ become zero, making L^I_{nn} only dependent on medium 1 and 2 (see eq 4). As a result, the ratio $|L^I_{nn,H_2O}(\omega_{IR})|^2/|L^I_{nn,D_2O}(\omega_{IR})|^2 \approx 1$. The Fresnel factor itself ($L^I_{nn,H_2O}(\omega_{IR})$) will still have a modest frequency dependence, because the refractive indices of medium 1 and 2 are slightly frequency dependent. For the case of a very thick metal(-oxide) layer the Fresnel factors for the second interface become very small due to the absorption of the IR light.

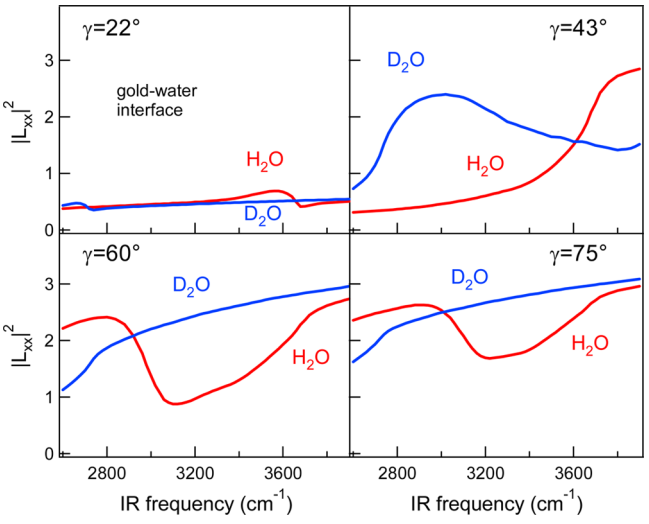

Figure 6. Square of the calculated IR Fresnel factors $|L_{xx}|^2$ for H_2O (red) and for D_2O (blue) for the gold–water interface measured for incident angles of 22, 43, 60, and 75°, illustrating that the frequency dependence mainly originates from the Fresnel factor of H_2O.

To predict relative signal sizes, the magnitude of the Fresnel factors has to be taken into account. Up to now, we only considered the spectral dependence of the signals that is determined by the dispersion of the IR light. To calculate the SFG amplitude we need to include the Fresnel factors at the SFG and visible frequencies, as can be seen in eq 3. We calculated the relative magnitudes of the signals for all systems and polarization combinations by using the refractive indices given in Table 2. The results are given in Table 3 and 4. For the IR light we used the Fresnel factor at 3300 cm^{-1}. Table 3 presents the calculation results for the case that the metal(-oxide) film is the nonlinear medium, while Table 4 presents the results for the case that sapphire or water forms the nonlinear medium. Of course the experimentally observed signals can be a sum of signals originating from the sapphire and metal(-oxide) media at the first interface and from the metal(-oxide) and water media at the second interface. Hence, in total there could be four contributions to the signal. For the PPP polarization combination there can even be 16 contributions: the four contributions from the different media enter in four different combinations of Fresnel factors (eq 3d).

Table 2. Real (n) and Imaginary Part (k) of the Refractive Index of the Different Materials Used in the Calculations Presented in Tables 3 and 4

	sapphire[44]		gold[44]		Ti[44]		ITO[47]		water[45,46]	
	n	k	n	k	n	k	n	k	n	k
IR 3300 cm^{-1}	1.709	0	1.67	18.79	2.55	4.35	0.55	3.60	1.409	0.243
VIS 12500 cm^{-1}	1.76	0	0.188	5.39	2.87	3.33	1.52	0.025	1.329	1.25×10^{-7}
SFG 15800 cm^{-1}	1.77	0	0.166	3.15	2.16	2.93	1.66	0.025	1.332	1.39×10^{-8}

Table 3. Calculated Magnitudes of the Fresnel Factors for the Case That Medium 2 (Thin Metal(-Oxide) Film) Is the Nonlinear Medium ($\chi^{(2)}_{medium2} > \chi^{(2)}_{water/sapphire}$)

	gold 5 nm				Ti 5 nm	ITO 100 nm
	22°	43°	60°	75°	45°	45°
sapphire−metal(-oxide) interface						
SSP: $\lvert L_{yy}(\omega_{SFG})L_{yy}(\omega_{VIS})L_{zz}(\omega_{IR})\sin\theta_{IR}\rvert^2$	1×10^{-4}	2×10^{-4}	5×10^{-5}	8×10^{-6}	0.01	0.44
SPS: $\lvert L_{yy}(\omega_{SFG})L_{zz}(\omega_{VIS})L_{yy}(\omega_{IR})\sin\theta_{VIS}\rvert^2$	3×10^{-3}	0.01	7×10^{-4}	4×10^{-5}	0.07	4.24
PSS: $\lvert L_{zz}(\omega_{SFG})L_{yy}(\omega_{VIS})L_{yy}(\omega_{IR})\sin\theta_{SFG}\rvert^2$	0.16	0.63	0.07	7×10^{-3}	2.46	2.74
PPP: $\lvert L_{xx}(\omega_{SFG})L_{xx}(\omega_{VIS})L_{zz}(\omega_{IR})\cos\theta_{SFG}\cos\theta_{VIS}\sin\theta_{IR}\rvert^2$	2×10^{-5}	2×10^{-6}	3×10^{-5}	9×10^{-6}	5×10^{-4}	1×10^{-4}
PPP: $\lvert L_{xx}(\omega_{SFG})L_{zz}(\omega_{VIS})L_{xx}(\omega_{IR})\cos\theta_{SFG}\sin\theta_{VIS}\cos\theta_{IR}\rvert^2$	1×10^{-3}	1×10^{-3}	9×10^{-4}	1×10^{-4}	5×10^{-3}	0.25
PPP: $\lvert L_{zz}(\omega_{SFG})L_{xx}(\omega_{VIS})L_{xx}(\omega_{IR})\sin\theta_{SFG}\cos\theta_{VIS}\cos\theta_{IR}\rvert^2$	0.08	0.13	0.19	0.03	0.19	0.02
PPP: $\lvert L_{zz}(\omega_{SFG})L_{zz}(\omega_{VIS})L_{zz}(\omega_{IR})\sin\theta_{SFG}\sin\theta_{VIS}\sin\theta_{IR}\rvert^2$	1×10^{-7}	3×10^{-6}	2×10^{-7}	1×10^{-8}	6×10^{-4}	0.32
metal(-oxide)-water interface						
SSP: $\lvert L_{yy}(\omega_{SFG})L_{yy}(\omega_{VIS})L_{zz}(\omega_{IR})\sin\theta_{IR}\rvert^2$	2×10^{-5}	7×10^{-5}	2×10^{-5}	3×10^{-6}	0.01	0.12
SPS: $\lvert L_{yy}(\omega_{SFG})L_{zz}(\omega_{VIS})L_{yy}(\omega_{IR})\sin\theta_{VIS}\rvert^2$	2×10^{-3}	0.01	2×10^{-3}	2×10^{-4}	0.07	1.47
PSS: $\lvert L_{zz}(\omega_{SFG})L_{yy}(\omega_{VIS})L_{yy}(\omega_{IR})\sin\theta_{SFG}\rvert^2$	0.40	1.99	0.29	0.03	7.64	2.39
PPP: $\lvert L_{xx}(\omega_{SFG})L_{xx}(\omega_{VIS})L_{zz}(\omega_{IR})\cos\theta_{SFG}\cos\theta_{VIS}\sin\theta_{IR}\rvert^2$	3×10^{-6}	3×10^{-6}	3×10^{-5}	6×10^{-6}	1×10^{-3}	2×10^{-3}
PPP: $\lvert L_{xx}(\omega_{SFG})L_{zz}(\omega_{VIS})L_{xx}(\omega_{IR})\cos\theta_{SFG}\sin\theta_{VIS}\cos\theta_{IR}\rvert^2$	7×10^{-4}	3×10^{-3}	4×10^{-3}	8×10^{-4}	8×10^{-3}	0.22
PPP: $\lvert L_{zz}(\omega_{SFG})L_{xx}(\omega_{VIS})L_{xx}(\omega_{IR})\sin\theta_{SFG}\cos\theta_{VIS}\cos\theta_{IR}\rvert^2$	0.20	0.79	1.06	0.21	0.93	0.36
PPP: $\lvert L_{zz}(\omega_{SFG})L_{zz}(\omega_{VIS})L_{zz}(\omega_{IR})\sin\theta_{SFG}\sin\theta_{VIS}\sin\theta_{IR}\rvert^2$	6×10^{-8}	6×10^{-6}	2×10^{-6}	2×10^{-7}	2×10^{-3}	0.17

Table 4. Calculated Magnitudes of the Fresnel Factors for the Case That Sapphire and/or Water Are the Nonlinear Medium ($\chi^{(2)}_{water/sapphire} > \chi^{(2)}_{medium2}$)

	gold 5 nm				Ti 5 nm	ITO 100 nm
	22°	43°	60°	75°	45°	45°
sapphire−metal(-oxide) interface						
SSP: $\lvert L_{yy}(\omega_{SFG})L_{yy}(\omega_{VIS})L_{zz}(\omega_{IR})\sin\theta_{IR}\rvert^2$	1.62	3.46	0.70	0.13	1.12	9.12
SPS: $\lvert L_{yy}(\omega_{SFG})L_{zz}(\omega_{VIS})L_{yy}(\omega_{IR})\sin\theta_{VIS}\rvert^2$	0.23	1.02	0.06	4×10^{-3}	2.68	2.36
PSS: $\lvert L_{zz}(\omega_{SFG})L_{yy}(\omega_{VIS})L_{yy}(\omega_{IR})\sin\theta_{SFG}\rvert^2$	0.02	0.06	7×10^{-3}	7×10^{-4}	0.14	3.51
PPP: $\lvert L_{xx}(\omega_{SFG})L_{xx}(\omega_{VIS})L_{zz}(\omega_{IR})\cos\theta_{SFG}\cos\theta_{VIS}\sin\theta_{IR}\rvert^2$	0.26	0.03	0.50	0.13	0.04	3×10^{-3}
PPP: $\lvert L_{xx}(\omega_{SFG})L_{zz}(\omega_{VIS})L_{xx}(\omega_{IR})\cos\theta_{SFG}\sin\theta_{VIS}\cos\theta_{IR}\rvert^2$	0.09	0.08	0.08	9×10^{-3}	0.18	0.14
PPP: $\lvert L_{zz}(\omega_{SFG})L_{xx}(\omega_{VIS})L_{xx}(\omega_{IR})\sin\theta_{SFG}\cos\theta_{VIS}\cos\theta_{IR}\rvert^2$	8×10^{-3}	0.01	0.02	3×10^{-3}	0.01	0.02
PPP: $\lvert L_{zz}(\omega_{SFG})L_{zz}(\omega_{VIS})L_{zz}(\omega_{IR})\sin\theta_{SFG}\sin\theta_{VIS}\sin\theta_{IR}\rvert^2$	0.02	0.44	0.03	2×10^{-3}	0.10	4.77
metal(-oxide)-water interface						
SSP: $\lvert L_{yy}(\omega_{SFG})L_{yy}(\omega_{VIS})L_{zz}(\omega_{IR})\sin\theta_{IR}\rvert^2$	0.61	2.07	0.58	0.10	1.80	5.22
SPS: $\lvert L_{yy}(\omega_{SFG})L_{zz}(\omega_{VIS})L_{yy}(\omega_{IR})\sin\theta_{VIS}\rvert^2$	0.48	3.96	0.54	0.06	7.91	2.52
PSS: $\lvert L_{zz}(\omega_{SFG})L_{yy}(\omega_{VIS})L_{yy}(\omega_{IR})\sin\theta_{SFG}\rvert^2$	0.02	0.06	7×10^{-3}	7×10^{-4}	0.14	0.99
PPP: $\lvert L_{xx}(\omega_{SFG})L_{xx}(\omega_{VIS})L_{zz}(\omega_{IR})\cos\theta_{SFG}\cos\theta_{VIS}\sin\theta_{IR}\rvert^2$	0.09	0.08	0.77	0.19	0.18	0.07
PPP: $\lvert L_{xx}(\omega_{SFG})L_{zz}(\omega_{VIS})L_{xx}(\omega_{IR})\cos\theta_{SFG}\sin\theta_{VIS}\cos\theta_{IR}\rvert^2$	0.20	0.85	1.07	0.21	0.98	0.38
PPP: $\lvert L_{zz}(\omega_{SFG})L_{xx}(\omega_{VIS})L_{xx}(\omega_{IR})\sin\theta_{SFG}\cos\theta_{VIS}\cos\theta_{IR}\rvert^2$	6×10^{-3}	0.03	0.03	7×10^{-3}	0.02	0.15
PPP: $\lvert L_{zz}(\omega_{SFG})L_{zz}(\omega_{VIS})L_{zz}(\omega_{IR})\sin\theta_{SFG}\sin\theta_{VIS}\sin\theta_{IR}\rvert^2$	0.01	1.44	0.41	0.06	0.58	5.15

In case the metal(-oxide) film constitutes the nonlinear medium (Table 3) all polarization combinations that involve $L_{zz}(\omega_{IR})$ yield very small SFG signals due to the large refractive index, especially the imaginary part, of the metal(-oxide) in the infrared region (see Table 2). This large refractive index is present in the denominator of the expression for $L_{zz}(\omega_{IR})$ thus making $L_{zz}(\omega_{IR})$ small. For PSS polarization combination the SFG signal is relatively large due to the large value of $L_{zz}(\omega_{SFG})$ that results from the small value of the refractive index of

sapphire and water in the visible (for $L_{zz}(\omega_{SFG})$, $n_{interface}$ is $n_{sapphire}$ or n_{water}).

In case the metal(-oxide) film is not the nonlinear medium the small values observed in Table 3 disappear (see Table 4). Now the SSP and SPS polarization combination yield large signals due to a large contribution from the $L_{zz}(\omega_{IR})$ and $L_{zz}(\omega_{VIS})$, respectively. In general, the PPP polarization combination gives smaller signals than the other polarization combination, because the expression for PPP includes a multiplication with two additional goniometric functions.

Comparison between Experiment and Calculations. As is clear from comparing the experimental and calculated spectra in Figures 3−5, the measured SFG spectra are always remarkably similar to at least one of the calculated squared ratios of the Fresnel factors.

For the PPP signal of gold (Figure 3) the experimentally observed ratio of the signals measured for H_2O and D_2O (Figure 3a) matches very well with the calculated ratio of the Fresnel factors $|L^{I}_{xx,H_2O}(\omega_{IR})|^2/|L^{I}_{xx,D_2O}(\omega_{IR})|^2$ and $|L^{II}_{xx,H_2O}(\omega_{IR})|^2/|L^{II}_{xx,D_2O}(\omega_{IR})|^2$ (red) for all four measured incident angles. Although the PPP signal is a combination of four terms of which two scale with $L^{n}_{xx}(\omega_{IR})$ and two with $L^{n}_{zz}(\omega_{IR})$, we do not observe a significant contribution from $L^{n}_{zz}(\omega_{IR})$. This observation can be understood by looking at the relative magnitude of the different signal contributions shown in Tables 3 and 4. Gold shows a very large nonlinear response (see, e.g., refs 18 and 19) meaning that we only need to consider the signal contributions from Table 3, i.e., the case that $\chi^{(2)}_{gold} > \chi^{(2)}_{water/sapphire}$. Moreover, if the nonlinear response of gold would have been small compared to that of water or sapphire, a large signal for the SSP polarization combination would have been observed, as is evident from Table 4. As we do not see a large signal for SSP, we can indeed conclude that the signal originates from the gold layer. Based on the Fresnel factors the largest contribution for PPP is then expected from the $|L^{II}_{zz}(\omega_{SFG})L^{II}_{xx}(\omega_{VIS})L^{II}_{xx}(\omega_{IR})|^2$ term (see Table 3), but a contribution from $|L^{I}_{zz}(\omega_{SFG})L^{I}_{xx}(\omega_{VIS})L^{I}_{xx}(\omega_{IR})|^2$ cannot be excluded, exactly the two factors that match very well the measured SFG spectrum. The relative magnitude of the observed signals for the different angles (i.e., large for 43 and 60°, small for 22 and 75°) is also in agreement with the calculations. Of course the tensor elements of $\chi^{(2)}_{ijk}$ also determine which contribution will be dominant in the signal. However, for PPP the term $|L^{II}_{zz}(\omega_{SFG})L^{II}_{xx}(\omega_{VIS})L^{II}_{xx}(\omega_{IR})|^2$ is in general over 1000 times larger than the other factors, whereas the $\chi^{(2)}_{ijk}$ tensor elements are in general not that different.[35]

For titanium (optical constants from ref 44) the experimental results are compared with the calculations in Figure 4. For the SSP polarization combination the data coincide with the ratios of the calculated IR Fresnel factors $|L^{I}_{zz,H_2O}(\omega_{IR})|^2/|L^{I}_{zz,D_2O}(\omega_{IR})|^2$ and $|L^{II}_{zz,H_2O}(\omega_{IR})|^2/|L^{II}_{zz,D_2O}(\omega_{IR})|^2$, whereas for the PSS polarization a good comparison of the data with the ratios of the calculated IR Fresnel factors $|L^{I}_{yy,H_2O}(\omega_{IR})|^2/|L^{I}_{yy,D_2O}(\omega_{IR})|^2$ and $|L^{II}_{yy,H_2O}(\omega_{IR})|^2/|L^{II}_{yy,D_2O}(\omega_{IR})|^2$ is found, as predicted by eq 3.[48] The measured PSS signal was much larger than the other signals. The calculation predict a strong signal for PSS when $\chi^{(2)}_{Ti} > \chi^{(2)}_{water/sapphire}$ (Table 3), hence the SFG signal appears to be generated by the titanium film. If water or sapphire would have been the nonlinear medium, a strong signal for the SPS combination would have been observed (see Table 4), which does not agree with the experimental observations. As for gold, the SFG signal originates from the metal rather than the water/sapphire. Both the first and second interface can contribute to the signal as the Fresnel factors for the two interfaces are comparable in size (see Table 3).

For ITO (Figure 5) the interpretation of the data is less straightforward than for gold and titanium. Unfortunately, we have no a priori knowledge about the relative magnitude of the nonlinear response of ITO compared to that of sapphire and water. The experimental data show that the SSP signal is roughly 6 times stronger than that obtained with PPP, and that the spectral shapes of the signals obtained with SSP and PPP are both similar to the frequency dependence of the ratio of the calculated IR Fresnel factors $|L^{II}_{zz,H_2O}(\omega_{IR})|^2/|L^{II}_{zz,D_2O}(\omega_{IR})|^2$. By comparing Table 3 and 4 we see that in both cases (ITO or sapphire/water as the nonlinear medium) the magnitudes of the Fresnel factors for SSP and PPP (the terms containing $L^{n}_{zz}(\omega_{IR})$) are comparable. In case water would be the dominant nonlinear medium, the *zzz* term of PPP will be dominant, in agreement with the observed correspondence of the signal with the spectral shape of $L^{II}_{zz}(\omega_{IR})$. However, as we did not observe any sign of a resonance in $\chi^{(2)}_{ijk}$ (no resonant water signal), it seems much more likely that the ITO film has a stronger nonlinear response than water, like the gold and titanium system. However, for the case that ITO is responsible for the SFG signal, the Fresnel factors associated with the *xzx*, *zxx*, and *zzz* terms of PPP are comparable in size. It will thus depend critically on the values of the corresponding $\chi^{(2)}_{ijk}$ tensor elements which Fresnel factor dominates.

Summarizing, for all three studied systems the experimental data can be fully explained by the shape and size of the Fresnel factors assuming that the SFG signal originates from the metal(-oxide) film. The nonresonant nonlinear response of the metal(-oxide) film is thus concluded to dominate the overall SFG response, although the infrared light is in resonance with the vibrations of water in the measured frequency range. The spectral dependence of the Fresnel factor is fully determined by the infrared field, due to the strong dispersion of the refractive index of water in this frequency region. Interestingly, different Fresnel factors dominate the response of the three studied systems, which can be explained from their specific IR, VIS, and SFG Fresnel factors. For gold in PPP polarization we find a good match of the signal with $|L^{I}_{xx,H_2O}(\omega_{IR})|^2/|L^{I}_{xx,D_2O}(\omega_{IR})|^2$ and $|L^{II}_{xx,H_2O}(\omega_{IR})|^2/|L^{II}_{xx,D_2O}(\omega_{IR})|^2$, indicated by the thick lines in Figure 3, panels b and c. For Ti the SSP measured data match well with $|L^{I}_{zz,H_2O}(\omega_{IR})|^2/|L^{I}_{zz,D_2O}(\omega_{IR})|^2$ and $|L^{II}_{zz,H_2O}(\omega_{IR})|^2/|L^{II}_{zz,D_2O}(\omega_{IR})|^2$, while for PSS $|L^{I}_{yy,H_2O}(\omega_{IR})|^2/|L^{I}_{yy,D_2O}(\omega_{IR})|^2$ and $|L^{II}_{yy,H_2O}(\omega_{IR})|^2/|L^{II}_{yy,D_2O}(\omega_{IR})|^2$ are observed (thick lines Figure 4, panels b and c). For ITO both in PPP and SSP polarization we observe a spectral dependence close to $|L^{II}_{zz,H_2O}(\omega_{IR})|^2/|L^{II}_{zz,D_2O}(\omega_{IR})|^2$ (thick line Figure 5c). The spectra of the metal(-oxide) interface films do not show any evidence for the presence of interfacial vibrational resonances in the second-order nonlinear susceptibility. The effect of the vibrational resonances only enters through the dispersion of the Fresnel coefficients for the infrared light, but these resonances are bulk water vibrations as the infrared light probes the water over its evanescent wavelength of several hundred nanometers.

CONCLUSIONS

We have analyzed surface sum-frequency generation (SFG) spectra obtained from supported thin metal and metal-oxide films in contact with water in an internal reflection configuration. We found that the shapes of the observed SFG spectra are completely dominated by the frequency-dependence of the Fresnel coefficients, which implies that the nonresonant SFG signal strongly dominates over the SFG signal of the vibrational resonances of the interfacial water molecules.

The results from the present study are important for future SFG studies on water at thin film metal and metal−oxide interfaces. For the study of the vibrational properties of interfacial species, it is advantageous to select experimental conditions in which the SFG Fresnel factors show little infrared frequency dependence. This can be achieved by decreasing the angle of incidence (see the angle dependence for gold in Figure 3). Smaller angles of incidence also allow for a deeper penetration of the beams across the thin metal layer. A disadvantage of choosing smaller angles of incidence is that the Fresnel factors become smaller because the system is further away from the surface plasmon resonance.[49] As a result the local electric fields and thus the generated SFG intensity decrease. Finally, to characterize the vibrational properties of interfacial water at interfaces, it is necessary to select a material which produces a much smaller nonresonant SFG signal (i.e., with a small nonresonant $\chi^{(2)}$) than the presently studied films. Even then, Fresnel factors will affect the shape of the SFG spectra (see eq 1), but the spectral structure of the SFG signal will not be completely dominated by the Fresnel factors and can thus be used to determine the frequency dependence of $\chi^{(2)}_{ijk}$ that reflects the vibrational modes of the interfacial species.

AUTHOR INFORMATION

Notes

The authors declare no competing financial interest.

ACKNOWLEDGMENTS

This work is part of the research program of the "Stichting voor Fundamenteel Onderzoek der Materie (FOM)", which is financially supported by the "Nederlandse organisatie voor Wetenschappelijk Onderzoek (NWO)". We gratefully acknowledge Y. Tong, P. Koelsch, and D. Verreault for stimulating scientific discussions, and H. Zeijlemaker and H. Schoenmaker for their technical support. N.G.A. acknowledges the European Commission (FP7) for the award of a Marie Curie fellowship.

REFERENCES

(1) Shen, Y. R. *Nature* **1989**, *337*, 519−525.
(2) Eisenthal, K. B. *Annu. Rev. Phys. Chem.* **1992**, *43*, 627−661.
(3) Eisenthal, K. B. *Chem. Rev.* **1996**, *96*, 1343−1360.
(4) Shultz, M. J.; Schitzer, C.; Simonelli, D.; Baldelli, S. *Int. Rev. Phys. Chem.* **2000**, *19*, 123−153.
(5) Richmond, G. L. *Annu. Rev. Phys. Chem.* **2001**, *52*, 357−389.
(6) Richmond, G. L. *Chem. Rev.* **2002**, *102*, 2693−2724.
(7) Tadjeddine, A. *Surf. Rev. Lett.* **2000**, *7*, 423−436.
(8) Vidal, F.; Tadjeddine, A. *Rep. Prog. Phys.* **2005**, *68*, 1095−1127.
(9) Wang, H. F.; Gan, W.; Lu, R.; Rao, Y.; Wu, B. H. *Int. Rev. Phys. Chem.* **2005**, *24*, 191−256.
(10) Campen, R. K.; Ngo, T. T. M.; Sovago, M.; Ruysschaert, J. M.; Bonn, M. *J. Am. Chem. Soc.* **2010**, *132*, 8037−8047.
(11) Chen, Z.; Shen, Y. R.; Somorjai, G. A. *Annu. Rev. Phys. Chem.* **2002**, *53*, 437−465.
(12) Lambert, A. G.; Davies, P. B.; Neivandt, D. J. *Appl. Spectrosc. Rev.* **2005**, *40*, 103−145.
(13) Bredenbeck, J.; Ghosh, A.; Smits, M.; Bonn, M. *J. Am. Chem. Soc.* **2008**, *130*, 2152−2153.
(14) Bonn, M.; Bakker, H. J.; Gosh, A.; Yamamoto, S.; Sovago, M.; Campen, R. K. *J. Am. Chem. Soc.* **2010**, *132*, 14971−14978.
(15) Shen, Y. R.; Ostroverkhov, V. *Chem. Rev.* **2006**, *106*, 1140−1154.
(16) Stiopkin, I. V.; Weeraman, C.; Pieniazek, P. A.; Shalhout, F. Y.; Skinner, J. L.; Benderskii, A. V. *Nature* **2011**, *474*, 192−195.
(17) Arnolds, H.; Bonn, M. *Surf. Sci. Rep.* **2010**, *65*, 45−66.
(18) Himmelhaus, M.; Eisert, F.; Buck, M.; Grunze, M. *J. Phys. Chem. B* **2000**, *104*, 576−584.
(19) Braunschweig, B.; Mukherjee, P.; Kutz, R. B.; Wieckowski, A.; Dlott, D. D. *J. Chem. Phys.* **2010**, *133*, 234702.
(20) Backus, E. H. G.; Kuiper, J. M.; Engberts, J. B. F. N.; Poolman, B.; Bonn, M. *J. Phys. Chem. B* **2011**, *115*, 2294−2302.
(21) Feller, M. B.; Chen, W.; Shen, Y. R. *Phys. Rev. A* **1991**, *43*, 6778−6792.
(22) Feng, R. R.; Guo, Y.; Lü, R.; Velarde, L.; Wang, H. F. *J. Phys. Chem. A* **2011**, *115*, 6015−6027.
(23) Lambert, A. G.; Neivandt, D. J.; Briggs, A. M.; Usadi, E. W.; Davies, P. B. *J. Phys. Chem. B* **2002**, *106*, 5461−5469.
(24) Li, G.; Dhinojwala, A.; Yeganeh, M. S. *J. Phys. Chem. C* **2011**, *115*, 7554−7561.
(25) McGall, S. J.; Davies, P. B.; Neivandt, D. J. *J. Phys. Chem. B* **2004**, *108*, 16030−16039.
(26) Tong, Y.; Zhao, Y.; Li, N.; Osawa, M.; Davies, P. B.; Ye, S. *J. Chem. Phys.* **2010**, *133*, 034704.
(27) Tong, Y.; Zhao, Y.; Li, N.; Ma, Y.; Osawa, M.; Davies, P. B.; Ye, S. *J. Chem. Phys.* **2010**, *133*, 034705.
(28) York, R. L.; Li, Y.; Holinga, G. J.; Somorjai, G. A. *J. Phys. Chem. A* **2009**, *113*, 2768−2774.
(29) Zhuang, X.; Miranda, P. B.; Kim, D.; Shen, Y. R. *Phys. Rev. B* **1999**, *59*, 12632−12640.
(30) Lu, X.; Clarke, M. L.; Li, D.; Wang, X.; Xue, G.; Chen, Z. *J. Phys. Chem. C* **2011**, *115*, 13759−13767.
(31) Shen, Y. R. *Annu. Rev. Phys. Chem.* **1989**, *40*, 327−350.
(32) Mizrahi, V.; Sipe, J. E. *J. Opt. Soc. Am. B* **1988**, *5*, 660−667.
(33) Hansen, W. N. *J. Opt. Soc. Am.* **1968**, *58*, 380−390.
(34) These equations are basically the same as in ref 26. However, Tong et al. miss a factor cos θ_3/cos θ_1 in eq 10a. Moreover, the term accounting for the phase difference between multiple reflected beams should read exp(i2Δ).
(35) Wang, F. X.; Rodríguez, F. J.; Albers, W. M.; Ahorinta, R.; Sipe, J. E.; Kauranen, M. *Phys. Rev. B* **2009**, *80*, 233402.
(36) Jackson, J. D. *Classical Electrodynamics*; John Wiley & Sons, Inc.: New York, 1999.
(37) In eqs 6 to 8 from Lu et al. (ref 30) the $e^{i\beta}$ term should be removed in our opinion. This phase term is already included in $e^{i\Delta}$.
(38) Osawa, M.; Kuramitsu, M.; Hatta, A.; Suetaka, W. *Surf. Sci.* **1986**, *175*, L787−L793.
(39) Verreault, D.; Kurz, V.; Howell, C.; Koelsch, P. *Rev. Sci. Instrum.* **2010**, *81*, 063111.
(40) Williams, C. T.; Yang, Y.; Bain, C. D. *Langmuir* **2000**, *16*, 2343−2350.
(41) Nihonyanagi, S.; Ye, S.; Uosaki, K.; Dreesen, L.; Humbert, C.; Thiry, P.; Peremans, A. *Surf. Sci.* **2004**, *573*, 11−16.
(42) Noguchi, H.; Okada, T.; Uosaki, K. *Faraday Discuss.* **2008**, *140*, 125−137.
(43) Lagutchev, A.; Hambir, S. A.; Dlott, D. D. *J. Phys. Chem. C* **2007**, *111*, 13645−13647.
(44) Palik, E. D. *Handbook of optical constants of solids* 1985.
(45) Bertie, J. E.; Ahmed, M. K.; Eysel, H. H. *J. Phys. Chem.* **1989**, *93*, 2210−2218.
(46) Hale, G. M.; Querry, M. R. *Appl. Opt.* **1973**, *12*, 555−563.
(47) Hjortsberg, A.; Hamberg, I.; Granqvist, C. G. *Thin Solid Films* **1982**, *90*, 323−326.

(48) As we can not exclude that the Ti layer is partly oxidized, we compared our results for Ti with calculations for TiO_2. We found that the result is qualitatively the same.
(49) Ham, E. W. M. v. d.; Vrehen, Q. H. F.; Eliel, E. R.; Yakovlev, V. A.; Valieva, E. V.; Kuzik, L. A.; Petrov, J. E.; Sychugov, V. A.; Meer, A. F. G. v. d. *J. Opt. Soc. Am. B* **1999**, *16*, 1146−1152.